Multiphysics Analysis Of An In-Core Fission Product Removal System For The Molten Salt Fast Reactor

Federico Scioscioli, Antonio Cammi, <u>Carolina Introini</u>, Stefano Lorenzi
Politecnico di Milano, Department of Energy
Via La Masa 34
20133, Milano, Italy
federico.scioscioli@mail.polimi.it, antonio.cammi@polimi.it, carolina.introini@polimi.it, stefano.lorenzi@polimi.it

ABSTRACT

This work deals with the in-core helium injection system proposed for the Molten Salt Fast Reactor (MSFR), whose stated purpose is the online removal of both gaseous and metallic fission products. In order to properly analyse this system, we add the capability to simulate production, transport, and mass transfer of an arbitrary number of gaseous fission products (GFPs) to a pre-existing multiphysics solver, built with the OpenFOAM suite. We aim at starting a comprehensive analysis of the bubbling system, focusing on GFPs, focussing on some operational and safety-related features. Investigations of the first kind include quantifying the efficiency of GFP removal through a characteristic removal time, estimating the poisoning effect of GFPs, and evaluating the activity and decay heat of the removed gas, an aspect which crucially enters the design of the off-gas unit. Among the safety-related studies, the developed multiphysics tool allows evaluating the void coefficient, determining upper bounds on the He flow-rate in order to avoid prompt supercriticality in case of loss of He injection. In addition, two different possible accidents are evaluated involving complete loss of He injection, and complete loss of He removal. Results show the relevance of the thermal-hydraulic behaviour in preventing prompt supercriticality in case of loss of He injection.

1   INTRODUCTION

The current concept for the Molten Salt Fast Reactor (MSFR) includes an in-core helium injection system for the removal of Fission Products (FPs), both metallic and gaseous ones, which may be deleterious in terms of neutron poisoning, salt chemistry, and in the metallic case, deposition.

For the analysis of the MSFR, different approaches have been followed to account for the dynamics of the reactor both from a neutronics and thermal–hydraulics point of view. The very first attempt featured the combination of a zero-dimensional approach for thermal–hydraulics and point-kinetics for neutronics [1]. Following this, newer models were developed, including finite-element multiphysics codes, with multi-group diffusion equations for neutronics and an incompressible single-phase solver for thermal–hydraulics [2], able to simulate simplified 2D models of the MSFR. As a final step, a complete 3D model of the reactor has been constructed, and a multiphysics solver has been developed [3], based on the OpenFOAM C++ library, capable to work in both 2D and 3D geometry. Neutronics can be addressed with either diffusion or SP3 transport models, including delayed neutrons and decay heat precursors transport, while the thermal–hydraulics module follows a Computational Fluid Dynamics (CFD) approach able to work both in single and two-phase conditions, and is therefore capable to take into account the presence of the He phase.

Very recently, a paper [5] appeared extending the above solver with a model of Gaseous Fission Products (GFPs) production, transport, and mass transfer. In absence of new experimental results, data from the Molten Salt Reactor Experiment (MSRE) in the 1960s were employed. Since the MSRE was a thermal reactor, the only available results were for Xe-135, which was therefore the only GFP considered in that work. In particular, the resulting solver was found to be able to reproduce analytical benchmarks pertaining to Xe-135 mass transfer, and was employed to provide values for the bubbling system cycle time. This is the decay time of an assumed exponential decay in the FP population, and has been used in depletion codes to simplify burnup calculations [4]. The cycle time thus quantifies the efficiency of the bubbling system in extracting FPs from the fuel mixture. Before [5], a preliminary estimate was given in the order of magnitude of tens of seconds, with a proposed reference value of 30 s [4].

Building on the above work, in this paper we start what aims to be a comprehensive analysis of the bubbling system in the MSFR, considering both operational and safety-related aspects. The first step of the work is the extension of the aforementioned solver [5] to be able to cope with GFPs other than Xe-135. Then we verify his estimate in terms of the cycle time and of GFP poisoning contribution, at least as far as our isotope selection is concerned, and evaluate the activity and decay heat of the removed gas. These two latter quantities are of crucial importance in the design of the off-gas unit, determining its radioprotection and cooling requirements.

About safety-related studies, our solver allows the evaluation of the void coefficient at various levels of void fraction. This is of utmost importance, since He bubbling is envisaged to take place in-core, so in case of a loss of He a positive reactivity injection would occur. In order to avoid prompt supercriticality in this kind of accident, it is necessary to limit the He flow-rate. In addition, we simulate two possible accidents involving the bubbling system: the aforementioned loss of He injection, and loss of He removal. In the first case, the results show how the thermal-hydraulic behaviour of the MSFR can avoid prompt supercriticality even in case the void feedback associated to He loss is itself higher than the circulating delayed fraction.

2 THE SOLVER

Our starting point is the solver developed in [3] for the neutronic and the thermal-hydraulic analysis of the MSFR and extended by [5] for the modelling of Xe-135. In particular, the solver can deal with two-phase flows and has been used to study the effect of the helium bubbling system on neutronics [3] and to provide estimates for the cycle time [5].

At each time step, first the thermal-hydraulics problem is solved, which includes updating the GFP populations, and then the neutronics one, including transport of neutron and decay heat precursors. Then, external iterations are performed. We now provide very brief descriptions of the individual subsolvers. The reader is referred to the original publications for all details not reported here.

2.1 Neutronics

After updating cross sections to take into account temperature and density variations, the solver solves the equations for neutron balance. A multigroup approach is employed for energy discretisation, with 6 energy groups, while for the angular part the solver allows for a choice between diffusion theory and Simplified P3 (SP3) approach [3]. In this work, the diffusion model is exclusively adopted to limit the computational effort. The presence of blanket and reflectors is taken into account through appropriate albedo boundary conditions. Groups

constants are generated with the Monte Carlo (MC) code Serpent-2 [6], using the JEFF-3.1.1 library. The user can select between a time-dependent simulation and an eigenvalue mode, which employs a power iteration routine to determine the effective multiplication factor.

The evolution and motion of neutron and decay heat precursors are determined through appropriate balance equations. We employ 8 neutron and 3 decay heat precursor groups.

2.2   Thermal-hydraulics

When considering the bubbing system, the MSFR calls for a two-phase system modelling from a thermal-hydraulics point of view having a liquid (i.e., molten salt) and a gaseous (i.e., He bubbles) phases. The solver addresses this using an Euler-Euler method, i.e., in addition to the usual balance equations for mass, momentum, and energy, volume fractions are introduced for the two phases, each one with a corresponding balance equation. Turbulence is modelled with a RANS approach, specifically, a variant of the k-ε model, and pressure is assumed to be common to both salt and He.

Momentum and energy transfer between the two phases are modelled through explicit source terms in the balance equations. The various effects, e.g., drag, lift, turbulent dispersion and virtual mass forces in the momentum case, are taken into account through empirical correlations. The modelling choices made in this work are the same as in [3], to which we refer for motivation and details.

2.3   GFP modelling

The modelling of GFPs is the part of the solver which had to be modified with respect to the one presented in [5]. More specifically, [5] only considered the nuclide Xe-135, a choice motivated by the exclusive availability in the literature of experimental data for this GFP due to the MSRE experience.. In such a system, Xe-135 poisoning was such a dominant factor to monopolise attention as far as GFPs were concerned. Nevertheless, the MSFR is a fast system, and it is therefore not a priori clear that Xe-135 should still dominate poisoning.

Indeed, thanks to results obtained by [7], we now know that Xe-135 is by no means a dominant poison in the MSFR. Calculations of cumulative fission yields and cross-sections, performed with the Monte Carlo code Serpent-2, for isotopes of Kr and Xe, seem to indicate that poisoning is dominated by the Xe isotopes from 131 to 136. Accordingly, these are the GFPs considered in the present work. Incidentally, the fact that only Xe isotopes appear enables us to employ the same correlations as in the MSRE, for mass transfer is not expected to be sensibly influenced by isotopic effects. Thus, we deemed it necessary to extend the solver of [5] to be able to cope with arbitrary GFPs, possibly including elements other than Xe. Our modelling approach is a straightforward generalisation of the one presented in [5], to which we refer for additional details.

Letting α_k denote the phase fraction of phase and the concentration of specie i in phase k, we can write a balance equation

$$\frac{\partial(\alpha_k C_{k,i})}{\partial t} + \nabla \cdot \left(\alpha_k u_k C_{k,i} \right) - \nabla \cdot \left(\alpha_k D_{k,i} \nabla C_{k,i} \right) = \dot{m}_{k,i} + S_{k,i} \tag{1}$$

Here u_k is the velocity of phase k, $D_{k,i}$ is the diffusion coefficient for specie i in phase k, $\dot{m}_{k,i}$ represents mass transfer, and $S_{k,i}$ is a source term. The experimental results from the MSRE

enter in the modelling of the $\dot{m}_{k,i}$ term. For this, we first eliminate $D_{k,i}$ in favour of the Schmidt number, $Sc_{k,i} = \frac{v_k}{D_{k,i}}$, and then model

$$\dot{m}_{k,i} = K_{k,i}a_{k,k\prime}\left(C_{k,i}^{\infty} - C_{k,i}\right) \tag{2}$$

Here, $a_{k,k\prime}$ is the interfacial exchange area with phase $k\prime$, $C_{k,i}^{\infty}$ is the interface saturation concentration, and $K_{k,i}$ is an appropriate mass transfer coefficient. We model $C_{k,i}^{\infty}$ with a Henry-like law, i.e.,

$$C_{k,i}^{\infty} = HC_{k\prime,i} \tag{3}$$

For the constant H we use the value $2.08 \cdot 10^{-4}$. For $K_{k,i}$, we switch to the Sherwood number, $Sh = \frac{K_{k,i}d_b}{D_{k,i}}$, with d_b characteristic bubble diameter, and then employ the Higbie correlation,

$$Sh = 1.13Re_b^{1/2}Sc^{1/2} \tag{4}$$

with Re_b Reynolds number referred to the bubble diameter.

Thus, the current solver allows the simulation of an arbitrary number of GFPs. Apart from nuclear properties, information about mass transfer is required, in the form of both a correlation for the Sherwood number, and a value for the Henry coefficient.

3   SIMULATIONS

3.1   Geometry

The geometry employed in this work is the one adopted in the past EVOL project [8], consisting in a 2D axial-symmetric cylinder. The choice of using a 2D geometry is due to computational constraints: the solver itself is capable of dealing with 3D models of the MSFR, and has indeed been used so. Pump and heat exchanger are not modelled explicitly. Instead, their presence is taken into account through appropriate source and sink terms in the momentum and energy equations.

The geometry is represented in Figure 1, with indications about bubbling system, pump, and heat exchanger. At the hot leg, a free surface is present to allow for system expansion. The computational mesh consists of a total of 22671 elements.

3.2   Bubbling system characterisation

We now come to the analysis of the GFP removal system. We divide our analyses in three parts, namely *i*) evaluating the efficiency of GFP removal, through the cycle time; *ii*) quantifying its effectiveness, in terms of the poisoning contribution of the removed GFPs; and *iii*) assessing the activity and decay heat of the removed gas, of crucial importance for the off-gas unit.

The cycle time is introduced as a decay constant in the GFP inventory. In principle, it is allowed to be time-dependent. As already mentioned, this approach is well-suited to burnup calculations, and has been employed in several such studies, with the suggested value of 30 s [4]. To evaluate it, we compare, at each time step, the flow-rate of GFPs leaving the core and the total mass of GFPs. The results, at various He flow-rates, are reported in Figure 2.
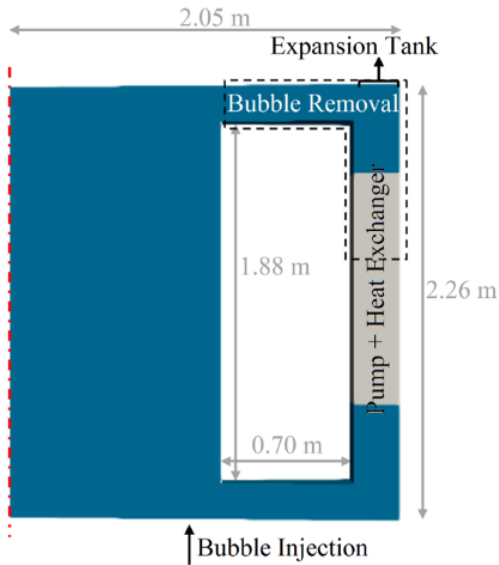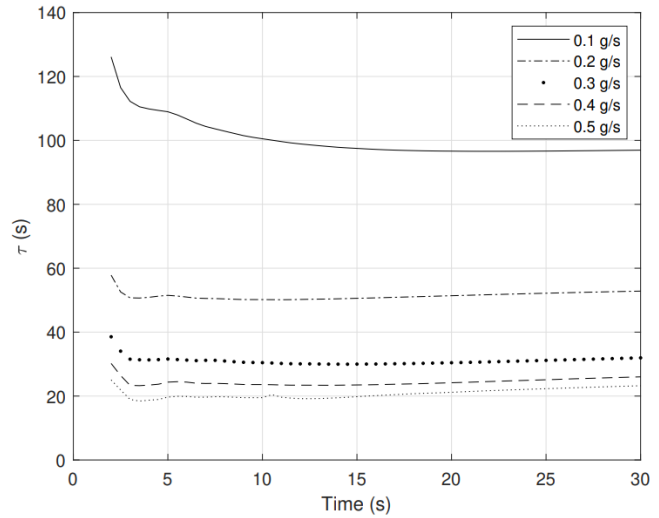
Figure 1: Computational geometry
Figure 2: Cycle time at various He flow-rates

As a general comment, these values are in very good agreement with those of [5], found by considering Xe-135 alone. We can see that, apart from an initial transient necessary for the He distribution in the core to stabilise, the cycle time approaches a constant, fully validating the assumption of an exponential decay. Moreover, this constant value is found to be inversely proportional to the He flow-rate, another result already present in [5]. We can also see that the value of 30 s, though quite optimistic, is at least of the correct order of magnitude.

Next, we evaluate the poisoning contribution of our isotope selection. In this respect, it is to be stressed that the current MSFR design does not include any control rod. Then, if the reactor is to be operated at constant temperature, some mechanism is required to cope with neutron poisoning. One possibility is to use the present bubbling system, while other proposals involve injecting fissile material. To compare the options, it is of importance to quantify the poisoning contribution of FPs.

Two different approaches are used. The first one consists in a single-phase calculation in eigenvalue mode, once including and once excluding the GFP terms from the neutronic problem. The second one calculates the variation of the multiplication factor upon removal, deactivating thermal feedback on cross-section and taking into account void variations with our values for the void coefficient, discussed in the next section. The results are nearly identical, confirming the soundness of the two approaches, and amount to about 38 pcm, or 0.3 $, for the GFP accumulated in a couple of weeks of operation without any removal. Incidentally, a similar calculation with Xe-135 alone gives 0.1 pcm, confirming that Xe-135 is here not a dominant poison at all.

Finally, we estimate the contribution of the removed FPs to the activity and decay heat of the gas leaving the core. This is of utmost importance, for these values determine the radioprotection and cooling requirements of the off-gas unit. Taking into account our GFP selection, and focussing on the radioactive ones, and referring again to a couple of weeks of operation without any removal, we find the values in Table 1, referred to the whole core. It should be evident that the off-gas unit will require some dedicated cooling system.

Table 1: Removed gas activity and decay heat

Isotope	Activity (Bq)	Decay heat (W)
Xe-133	$8.85 \cdot 10^{17}$	$2.55 \cdot 10^4$
Xe-135	$1.14 \cdot 10^{18}$	$1.03 \cdot 10^5$
Total	$2.03 \cdot 10^{18}$	$1.28 \cdot 10^5$

3.3 Safety-related studies

The introduction of the bubbling system clearly affects the whole reactor. In particular, the presence of a second in-core phase will have huge consequences on both neutronics and thermal-hydraulics, so that a safety analysis is necessary. Here, we focus on the effects on neutronics. The MSFR, like most existing or proposed reactors, presents a negative void coefficient. However, the adoption of bubbling in-core introduces a void fraction in normal operation not directly related with the power level. Then, a loss of He represents a possible reactivity accident mechanism.

Thus, first of all we quantify the void coefficient at various levels of void fraction. This translates in an upper limit on the He flow-rate, in order to avoid prompt supercriticality in case of loss of injection. Then, we simulate the transients following loss of He injection and of He removal. From the analysis of the first one, it will be clear that the thermal-hydraulic behaviour of the MSFR is of importance in avoiding prompt supercriticality even in case the void feedback exceeds the delayed fraction.

To find the void coefficient, we work in eigenvalue mode, injecting He in an initially single-phase core, with all terms related to GFPs removed from the neutronics problem. The results are in Table 2. Values of He flow-rate are here referred to the simulated geometry. When properly converted, we find an upper limit of about 0.3 g/s per core sector in order to avoid a void feedback higher than the delayed fraction. For the common range of He flow-rate, these values agree, within 10%, with those found in [3] through several independent means, and are consistent with the limiting value of -160 pcm/% obtained in [3] for a uniform bubble distribution.

Table 2: Void fraction and void coefficient

He flow-rate (g/s)	Void fraction (%)	Void coefficient (pcm/%)
0.1	0.69	-293
0.2	1.8	-245
0.3	3.2	-218
0.4	5.0	-192
0.5	6.9	-187

We next consider the two accidents mentioned above: complete loss of He injection, and complete loss of He removal. Loss of injection will be more severe, since it will decrease the void fraction, injecting positive reactivity into the system, while loss of removal will increase the void fraction without limit, shutting down the reactor. The accidents are modelled as steps at time 0, starting from stationary two-phase conditions for the nominal He and salt flow-rate. The plots are in Figures 3 and 4.

Starting from loss of injection, we find that power attains a maximum at about +80% of the nominal value in a few seconds. Then, thermal feedback intervenes, stabilising the power at about +40% after 10 s. Of particular interest is that, based on considerations of void feedback alone, the reactor should go prompt supercritical, i.e., if all bubbles were to disappear at time 0, prompt supercriticality would be reached. Since this is not observed, we conclude that the transient is slow enough for the temperature feedback to intervene, thus avoiding prompt supercriticality.

In case of loss of removal, equilibrium will not be reached: since injection is assumed to continue, the void fraction will keep increasing until complete shutdown. We observe that there is a delay in power reduction of a few seconds. This can be explained as a geometrical effect, since the gas about to be removed will be forced to flow through the circulation loop, where neutron importance is low, before re-entering the core from below, thus contributing to the shutdown. Also notice that this same effect will sharply increase the void fraction in the pump region, possibly bringing damage.
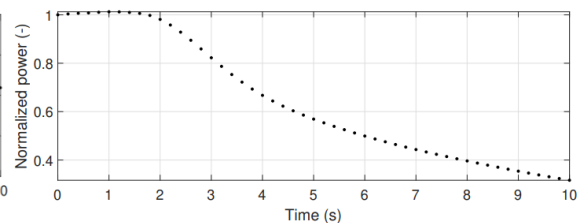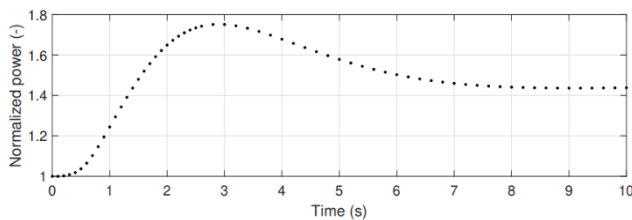

Figure 3: Power following loss of injection   Figure 4: Power following loss of removal

4   CONCLUSIONS

The work presented in this paper extends the capabilities of MSFR multiphysics tools in analysing the behaviour of GFPs. In particular, production, transport, consumption and removal by the bubbling system are all considered for an arbitrary GFP selection, the one employed in this paper having been chosen due to its expected poisoning contribution. Apart from nuclear properties, information for mass transfer is required in terms of a correlation for the Sherwood number and a value for the Henry coefficient.

The resulting solver is employed in the analysis of the bubbling system, both for its characterisation and for safety-related studies. In particular, we derive upper limits on the He flow-rate to avoid prompt supercriticality in case of accidents. However, we also show that the MSFR thermal-hydraulic behaviour tends to avoid prompt supercriticality even in case the reactivity associated to the void feedback exceeds the delayed fraction. We also estimate the source term due to the gas leaving the core, showing that a dedicated cooling system will definitely be required.

Further developments on the study of the bubbling system may make use of the solver presented here to analyse its effects on the MSFR. However, we stress that different models and correlations should be tested for mass transfer, and the selection of GFPs should be more carefully chosen. Finally, the effects of bubbling on metallic FPs should be investigated.

DISCLAIMER

The context of this paper does not reflect the official opinion of the European Union. Responsibility for the information and/or views expressed therein lies entirely with the authors.

REFERENCES

[1] Cammi, A. et al.,"Transfer Function Modeling of Zero-Power Dynamics of Circulating Fuel Reactors", J. Eng. Gas Turbines Power, 133, 2011

[2] Fiorina, C. et al., "Modelling and analysis of the MSFR transient behaviour", Ann. Nucl. Energy 64, 485–498, 2014

[3] Cervi, E., Lorenzi, S., Cammi, A., Luzzi, L., "Development of a multiphysics model for the study of fuel compressibility effects in the Molten Salt Fast Reactor", Chemical Engineering Science, 193, 379-393, 2019

[4] Aufiero, M. et al., "An extended version of the SERPENT-2 code to investigate fuel burn-up and core material evolution of the Molten Salt Fast Reactor", J. Nucl. Mater. 441, 473–486, 2013

[5] Caruggi, F. et al.,"Multiphysics modelling of gaseous fission products in the Molten Salt Fast Reactor", Nuclear Engineering and Design, 392, 2022

[6] Leppanen, J. et al., "The Serpent Monte Carlo code: status, development and applications in 2013", Ann. Nucl. Energy 82, 142–150, 2015

[7] Merla, G., Cammi, A., Lorenzi, S., "A New Reactivity Control Approach for Circulating Fuel Reactors", Proc. Int. Conf. Nuclear Energy for New Europe, Bled, Slovenia, September 6-9, Nuclear Society of Slovenia, 2021.

[8] Brovchenko, M., Merle Lucotte et al., "Optimization of the pre-conceptual design of the MSFR", Deliverable 2, 1–69, 2013